

## ORIGINAL ARTICLE

# Investigation of Cherenkov Radiation-Induced Hyperthermia in Radionuclide Therapy for Liver Cancer

Hadi Rezaei<sup>1</sup>, Babak Mahmoudian<sup>2,3</sup>, Asra Sadat Talebi<sup>2,4\*</sup> 

<sup>1</sup> Department of Radiology, School of Paramedical Sciences, Shiraz University of Medical Sciences, Shiraz, Iran

<sup>2</sup> Medical Radiation Sciences Research Center, Tabriz University of Medical Sciences, Iran

<sup>3</sup> Department of Nuclear Medicine, Tabriz University of Medical Sciences, Tabriz, Iran

<sup>4</sup> Department of Medical Physics, Medical School, Tabriz University of Medical Sciences, Tabriz, Iran

\*Corresponding Author: Asra Sadat Talebi

Received: 16 December 2025 / Accepted: 26 December 2025

Email: [Asra.talebi@yahoo.com](mailto:Asra.talebi@yahoo.com)

## Abstract

**Purpose:** Beta-emitting radionuclides used in liver cancer therapy generate cytotoxic effects and Cherenkov radiation. This study aims to evaluate the potential of Cherenkov radiation to induce localized hyperthermia in hepatic tumors during radionuclide therapy.

**Materials and Methods:** Monte Carlo simulations were performed using the GATE platform to model Cherenkov radiation transport and heat deposition in hepatic tumor tissue. The absorbed thermal dose was quantified using the integrated bioheat transfer model, allowing accurate voxel-level mapping of temperature distribution. Six beta-emitting radionuclides, including <sup>32</sup>P, <sup>90</sup>Y, <sup>166</sup>Ho, <sup>188</sup>Re, <sup>177</sup>Lu, and <sup>131</sup>I, were evaluated to assess their potential for inducing thermal effects through Cherenkov radiation absorption during liver radionuclide therapy.

**Results:** Among the radionuclides studied, <sup>32</sup>P and <sup>90</sup>Y generated the highest number of Cherenkov photons in the liver tumor, resulting in significant heat deposition and uniform tumor temperatures ranging from 41 to 49°C, consistent with mild hyperthermia and, in the case of <sup>32</sup>P, partial thermal ablation with approximately 20% of the tumor volume exceeding 60°C. <sup>166</sup>Ho induced moderate heating, raising tumor temperatures to around 41°C in most of the tumor volume. In contrast, radionuclides with lower beta energies, such as <sup>177</sup>Lu, <sup>131</sup>I, and <sup>188</sup>Re, produced minimal Cherenkov photon emission, resulting in negligible thermal effects within the tumor.

**Conclusion:** The integration of radionuclide therapy with Cherenkov radiation-induced hyperthermia presents a promising strategy for radiosensitization and thermal ablation in hepatocellular carcinoma.

**Keywords:** Radionuclide; Hyperthermia; Cherenkov Radiation; Liver Cancer.

## 1. Introduction

Radionuclide therapy for liver cancer is a form of targeted radiotherapy designed to deliver potent radiation directly to malignant hepatic lesions via the arterial circulation [1]. This approach takes advantage of the distinct vascular supply of liver tumors, which primarily receive blood from the hepatic artery, unlike the surrounding healthy liver tissue, predominantly supplied by the portal vein. Introducing radioactive compounds into this arterial system enables maximizing radiation delivery to tumor sites while minimizing exposure to normal tissue [2]. Various therapeutic radionuclides, primarily beta emitters, have been developed for this purpose, including  $^{90}\text{Y}$ ,  $^{131}\text{I}$ ,  $^{188}\text{Re}$ ,  $^{32}\text{P}$ ,  $^{177}\text{Lu}$ , and  $^{166}\text{Ho}$ , each selected based on its radiophysical properties and clinical indications [3].  $^{90}\text{Y}$ , in particular, is widely utilized in the form of microspheres for both primary liver cancer, such as hepatocellular carcinoma, and secondary tumors originating from other organs [4].

As beta-emitting radionuclides decay within biological tissues such as the liver, they emit energetic beta particles that travel through the surrounding medium. As these charged particles pass through the tissue, they deposit energy primarily by ionizing nearby atoms and molecules, especially water. This ionization process generates highly reactive free radicals, which cause indirect biological damage by attacking critical cellular components such as Deoxyribonucleic acid (DNA), proteins, and lipids [5, 6]. Alongside this indirect damage, beta particles can also directly break chemical bonds within DNA strands. The combined burden of direct ionization and oxidative stress often exceeds the capacity of the cell's repair systems, ultimately resulting in programmed cell death (apoptosis) or uncontrolled cell destruction (necrosis) [7].

In addition to causing biological damage, traversing tissue by high-energy beta particles can lead to a distinctive physical phenomenon known as Cherenkov radiation. When these beta particles exceed the speed of light in the biological medium, which is determined by the tissue's refractive index, they induce polarization in surrounding molecules. As the molecules return to their ground state, they emit dim, continuous light spanning the Ultraviolet (UV) to visible regions, with its maximum intensity in the UV

[8]. Many therapeutic radionuclides, being high-energy beta emitters, routinely exceed the energy threshold for Cherenkov emission in soft tissues (typically 213–219 keV). Consequently, they serve as effective internal sources of Cherenkov light [9]. The yield of this radiation depends on both the medium's refractive index and the radionuclide's beta energy spectrum [10]. Although the relatively low photon yield and strong absorption of UV/blue light in tissues remain key limitations, Cherenkov radiation has enabled promising innovations in medical applications, including intraoperative tumor visualization, radiotherapy guidance, and photodynamic therapy using internally generated light [11].

In organs like the liver, which exhibit relatively high optical absorption coefficients, particularly in the UV-to-blue spectral range, a significant fraction of these Cherenkov photons can be absorbed locally [12]. This absorption may lead to localized tissue heating, potentially inducing mild hyperthermia during radionuclide therapy. Cancer cells show signs of apoptosis when exposed to temperatures of 41–45°C, and protein denaturation occurs at temperatures exceeding 50°C, leading to irreversible cellular damage [13]. Despite the potential importance of this phenomenon, no studies to date have quantified the heat deposited in hepatic tumors via Cherenkov radiation absorption during radionuclide therapy. To address this gap, we propose using Monte Carlo simulations, which provide detailed, accurate modeling of photon transport and absorption in heterogeneous tissues. This approach surpasses analytical methods by accounting for the complex geometries and variable optical properties of biological tissues, making it a powerful tool for estimating spatially resolved thermal distributions within tumors. The primary purpose of this study is to quantitatively evaluate the potential of Cherenkov radiation to induce localized hyperthermia in hepatic tumors during radionuclide therapy using Monte Carlo simulations.

## 2. Materials and Methods

### 2.1. Simulation Framework

GATE (GEANT4 Application for Tomographic Emission) Monte Carlo code (version 9.1), based on the GEANT4 (Geometry and Tracking) toolkit (version 10.7.2), was employed to model photon transport, Cherenkov photon propagation, and subsequent heat deposition in biological tissues [14, 15]. Unlike analytical models, GATE enables detailed, realistic simulation of complex tissue geometries, such as liver parenchyma. Its flexibility and accuracy make it particularly suitable for biomedical thermal simulations. The validity of this approach has been demonstrated in previous studies, including that of Cuplov *et al.* [16]. Electromagnetic interactions were described using the Livermore physics list, with a secondary-particle production threshold of 0.1 mm to ensure accurate energy-deposition tracking [17]. Optical processes, including absorption, Rayleigh scattering, boundary interactions, and Cherenkov emission, were fully implemented to capture photon behavior within tissue structures [18, 19].

### 2.2. Phantom Geometry and Optical Properties

An adult female XCAT phantom was used to represent human anatomical structure [20]. A tumor with a volume of 14310 mm<sup>3</sup> was embedded within the liver region of the phantom (matrix dimensions: 240 × 240 × 540; voxel size: 3 × 3 × 3 mm<sup>3</sup>). Optical parameters of the liver tissue, including refractive index, absorption coefficient, and scattering coefficient, were obtained from experimental studies and incorporated into the model [21]. The selected radionuclides were uniformly distributed throughout the tumor volume, with their decay properties extracted from the MIRD (Medical Internal Radiation

Dose) database [22]. The physical properties of the radionuclides used are summarized in Table 1.

### 2.3. Heat Deposition Modeling

The heat absorbed in liver tissue was quantified using a hybrid modeling strategy that combines Monte Carlo-based radiation transport with an analytical solution of the Pennes bioheat equation. This model remains the cornerstone of thermal analysis in perfused biological tissues, as it incorporates conductive heat transfer, perfusion-mediated thermal dissipation, and localized energy deposition from Cherenkov radiation [16]. The governing equation for heat transfer in perfused tissues is described by [23, 24] (Equation 1):

$$\frac{\partial T(x,y,z,t)}{\partial t} = \frac{k}{\rho c} \nabla^2 T(x,y,z,t) + \frac{p_b c_b}{\rho c} w_b [T_a(x,y,z,t) - T(x,y,z,t)] + Q(x,y,z,t) \quad (1)$$

Where:  $T(x,y,z,t)$  represents the local tissue temperature at position  $(x,y,z)$  and time  $t$ ,  $\rho$ ,  $c$  and  $k$  are the tissue's density, specific heat capacity, and thermal conductivity, respectively.  $p_b c_b$ , and  $w_b$  correspond to blood density, specific heat, and perfusion rate, respectively.  $T_a$  denotes the arterial blood temperature.  $Q(x,y,z,t)$  is the volumetric energy deposition from Cherenkov radiation.

This study extracted the spatial distribution of deposited energy ( $Q(x,y,z,t)$ ) from Monte Carlo simulations conducted using the GATE platform. This energy map served as the initial condition for calculating the temperature distribution across the tissue. The analytical solution to the Pennes equation, suitable for this scenario, is given by [16] (Equation 2):

$$T(x,y,z,t) = [T(x,y,z,0) - T_a] \otimes G(x,y,z,t) \cdot e^{-\beta t} + T_a \quad (2)$$

**Table 1.** Main physical properties of the selected radionuclides

Radionuclide	(Major) Decay mode	Half-Life(days)	$E_{\beta\text{mean}}$ (MeV)	$E_{\beta\text{max}}$ (MeV)(%abundance)
Y-90	$\beta^-$	2.66	0.926	2.284 (100)
P-32	$\beta^-$	14.30	0.695	1.710(100)
Re-188	$\beta^-$	0.70	0.764	2.118(72)
Ho-166	$\beta^-$	1.13	0.666	1.840 (50.5)
Lu-177	$\beta^-$	6.64	0.133	0.497 (79)
I-131	$\beta^-$	8.02	0.192	0.606(89)

Where:  $G(x,y,z,t)$  represents a three-dimensional Gaussian distribution accounting for thermal diffusion over time.  $\alpha = \frac{k}{\rho c}$  is the thermal diffusivity of the tissue.  $\beta = \frac{p_b c_b w_b}{\rho c}$  incorporates the effect of blood perfusion as an exponential decay.

The heat diffusion process was implemented in the GATE Monte Carlo code using the ThermalActor, with thermal propagation modeled through convolution operations via the Insight Segmentation and Registration Toolkit [25]. To capture the temporal dynamics of heat diffusion, the simulation was discretized into multiple time frames using the setNumberOfTimeFrames parameter. The cumulative thermal distribution was reconstructed by summing the individual diffused frames, yielding a comprehensive voxelized map of the temperature rise over the entire decay period of the radionuclides. This combined Monte Carlo–analytical framework enabled high-fidelity estimation of both spatial and temporal heat distributions within the tumor, providing detailed insight into thermal effects during radionuclide therapy mediated by Cherenkov radiation. The absorbed heat in tumor tissue due to Cherenkov radiation in the 200-1000 nm wavelength range was quantified using the ThermalActor. The statistical uncertainty of the Monte Carlo simulations was controlled by employing  $10^9$  primary particle histories for each radionuclide. Under these conditions, the relative statistical uncertainty in the estimated number of Cherenkov photons and absorbed heat was below 2%. Comparisons between radionuclides were therefore based on differences exceeding the Monte Carlo statistical uncertainty, allowing meaningful discrimination of photon yields without the use of conventional hypothesis-based statistical tests.

### 3. Results

This study calculated the Cherenkov radiation spectrum within tumoral tissue in the presence of various beta-emitting radionuclides. Figure 1 shows the number of Cherenkov photons for different radionuclides within the tumor. The number of Cherenkov photons generated within the hepatic tumor in the presence of  $^{32}\text{P}$  was significantly higher than that of the other investigated radionuclides. In contrast,  $^{177}\text{Lu}$  exhibited the lowest Cherenkov

photon yield in the tumoral tissue. The mean energy of Cherenkov photons within the tumor remained constant across all radionuclides at 3.9 eV.

Figure 2 illustrates the Thermal Volume Histograms (TVH) of tumoral and non-tumoral liver tissues during radionuclide therapy with various radionuclides. Following the absorption of Cherenkov radiation emitted by  $^{32}\text{P}$ , the tumor volume increased in temperature to approximately  $49^\circ\text{C}$ . For  $^{90}\text{Y}$ , the temperature in 100% of the tumor volume reached  $44^\circ\text{C}$ . In the case of  $^{166}\text{Ho}$ , about 90% of the tumor volume reached  $41^\circ\text{C}$ . No notable temperature rise was observed in the tumoral liver tissue for the other investigated radionuclides. Furthermore, according to the TVHs, no significant temperature changes were detected in the non-tumoral liver tissue.

Figure 3 presents the two-dimensional temperature distribution in the liver tissue and the corresponding temperature profiles resulting from the absorption of Cherenkov radiation emitted by different radionuclides. During radionuclide therapy with  $^{32}\text{P}$ , the mean temperature within the tumoral liver tissue was markedly higher than that of the other radionuclides. In contrast, radionuclide therapies with  $^{177}\text{Lu}$ ,  $^{188}\text{Re}$ , and  $^{131}\text{I}$  showed no significant temperature changes in tumor tissue. The findings demonstrated in Figures 2 and 3 are consistent and mutually reinforcing. The thermal volume histograms in Figure 2 quantitatively illustrate the extent of temperature elevation across the tumor volume. In contrast, the two-dimensional temperature maps and profiles in Figure 3 reveal the spatial localization and heterogeneity of the same thermal effects. Both figures

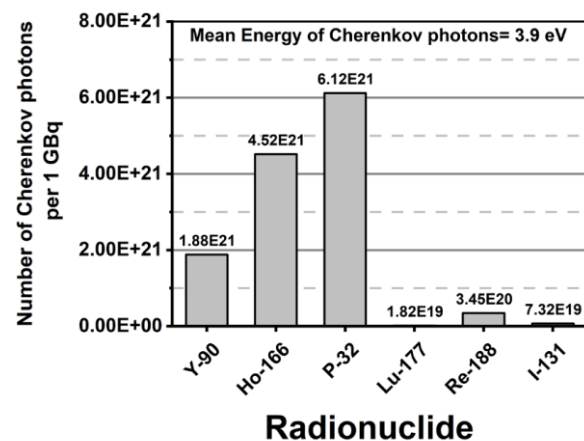
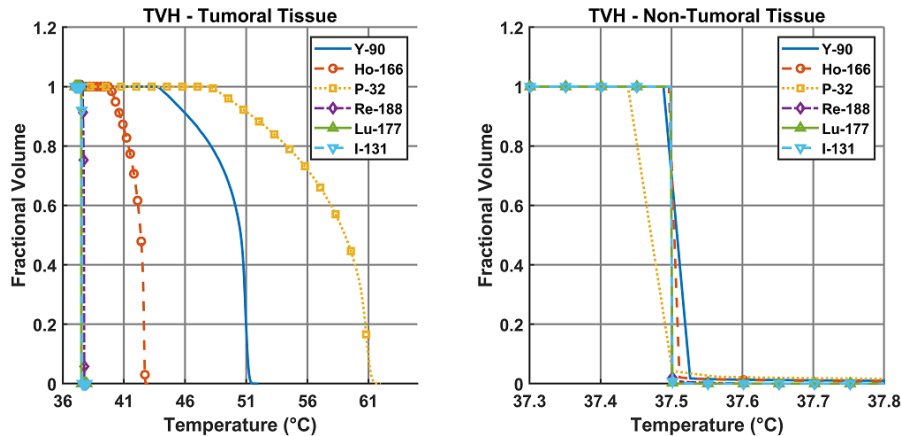
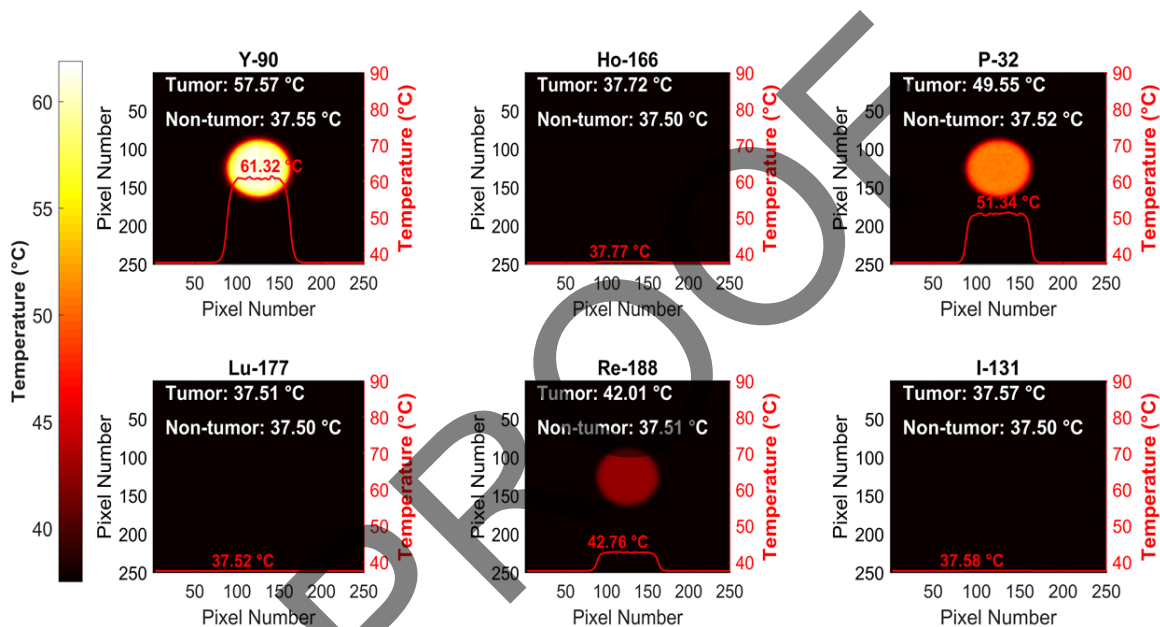


Figure 1. The number of Cherenkov photons for different radionuclides within the tumoral tissue



**Figure 2.** The TVHs of tumoral and non-tumoral liver tissues during radionuclide therapy with various radionuclides



**Figure 3.** Two-dimensional temperature distribution and temperature profiles in the liver tissue during radionuclide therapy with various radionuclides

consistently indicate pronounced tumor heating with  $^{32}\text{P}$  and  $^{90}\text{Y}$  and negligible temperature changes with radionuclides of lower beta energy, thereby supporting the same overall conclusions regarding Cherenkov radiation-induced hyperthermia.

#### 4. Discussion

This is the first study to use Monte Carlo simulations to explore Cherenkov radiation-induced hyperthermia in hepatic tumor radionuclide therapy with different beta-emitting radionuclides. Monte Carlo simulation offers advantages over traditional thermal modeling approaches when accurately

predicting temperature increases in biological tissues [15, 18]. While commonly used software platforms like COMSOL Multiphysics rely on simplified models such as the diffusion approximation or the Kubelka-Munk model [26]. COMSOL models photon transport using the diffusion approximation, which assumes that the scattering coefficient is much greater than the absorption coefficient. This assumption is often invalid in biological tissues, thereby reducing the accuracy of simulations of light and heat distribution. As a result, the software may underestimate localized heat deposition during phototherapy [27]. In contrast, Monte Carlo methods trace the path of individual photons and their interactions with tissue structures, providing a much more accurate estimation of energy

deposition. Based on the Geant4 Monte Carlo toolkit, the GATE platform is particularly well-suited for this purpose, as it allows detailed, voxel-based modeling of radiation transport and heat generation [14, 16]. This level of precision is essential for evaluating localized temperature increases induced by Cherenkov radiation during radionuclide therapy.

According to the Frank-Tamm formula, the frequency of Cherenkov radiation in a medium depends on both the energy of the emitted beta particles and the refractive index of the surrounding medium [28]. In a study by Gill *et al.*, the Cherenkov photon yield per disintegration was calculated for various beta-emitting radionuclides. Based on their findings,  $^{90}\text{Y}$  exhibited the highest Cherenkov yield per disintegration due to its higher beta energies [9]. However, our study showed that the total number of Cherenkov photons generated within hepatic tumor tissue per 1 GBq of activity during radionuclide therapy was significantly higher with  $^{32}\text{P}$  than with the other radionuclides. Although  $^{90}\text{Y}$  has a higher Cherenkov yield per disintegration, the number of disintegrations occurring in one GBq of  $^{32}\text{P}$  is approximately 5.7 times greater than that of  $^{90}\text{Y}$ . This higher disintegration per unit activity accounts for the greater Cherenkov photon production observed in  $^{32}\text{P}$ -based radionuclide therapy. For radionuclides such as  $^{177}\text{Lu}$  and  $^{131}\text{I}$ , the total number of Cherenkov photons generated per 1 GBq of activity was considerably lower due to their lower beta energies and reduced Cherenkov photon yields [22]. A positive correlation exists between the number of Cherenkov photons generated and the magnitude of the induced heat, as tissue heating arises from their absorption. Nevertheless, this relationship is not strictly linear. The effective heat deposition depends on additional factors, including the photon energy distribution, tissue optical absorption, and physiological heat-dissipation mechanisms, such as blood perfusion and thermal conduction. As a result, a high Cherenkov photon yield is a necessary but not sufficient condition for substantial temperature elevation.

Due to the high absorption coefficient of liver tissue [29, 30], Cherenkov radiation emitted by beta-emitting radionuclides such as  $^{32}\text{P}$  and  $^{90}\text{Y}$  can induce localized heating within tumoral regions. Our results demonstrated that during radionuclide therapy with  $^{32}\text{P}$

and  $^{90}\text{Y}$ , 100% of the tumor volume reached temperatures between 41°C and 45°C, fulfilling the criteria for mild hyperthermia. Mild hyperthermia in this range is known to disrupt tumor metabolism, impair DNA repair, and enhance tumor sensitivity to chemotherapy and radiotherapy [31, 32]. Additionally, approximately 100% and 90% of the tumor volume reached around 46°C in  $^{32}\text{P}$  and  $^{90}\text{Y}$  therapies, respectively, indicating a transition into temperature ranges associated with direct thermal damage to tumor cells via protein denaturation and membrane disruption [33]. Notably, in  $^{32}\text{P}$  therapy, nearly 20% of the tumor volume exceeded 60°C, reaching thermal ablation thresholds associated with immediate and irreversible tumor necrosis [34, 35]. These findings suggest that Cherenkov radiation-induced hyperthermia, especially in radionuclide therapy using high-energy beta emitters, may be a complementary mechanism for enhancing therapeutic efficacy. This effect was less pronounced in radionuclide therapies involving  $^{166}\text{Ho}$ , where only moderate heating (up to ~42°C) was observed, and virtually absent in therapies with  $^{177}\text{Lu}$ ,  $^{188}\text{Re}$ , and  $^{131}\text{I}$ , due to their lower beta energies and limited Cherenkov photon production. Several key factors govern the efficiency of heat generation through Cherenkov radiation absorption. These include the physical properties of the radionuclide, such as the beta particle energy spectrum, Cherenkov photon yield, and physical half-life, which determine the total number of emitted photons. In addition, tissue-specific optical properties, particularly the refractive index and optical absorption coefficient, strongly influence the fraction of Cherenkov photons absorbed locally. Finally, thermal and physiological parameters, including blood perfusion, thermal conductivity, and tissue heat capacity, regulate heat dissipation and ultimately control the magnitude and spatial distribution of the resulting temperature rise.

Numerous preclinical and clinical studies have shown that combining radiation and hyperthermia yields a synergistic effect, particularly when both modalities are applied simultaneously [36-38]. It is important to emphasize that the therapeutic effectiveness of heat-induced treatment is not directly comparable to that of radionuclide therapy in terms of absorbed radiation dose. Radionuclide therapy primarily induces tumor cell death through ionizing radiation-mediated DNA damage. In contrast,

hyperthermia exerts its biological effects via distinct mechanisms, including protein denaturation, membrane destabilization, inhibition of DNA repair processes, and modulation of the tumor microenvironment. Accordingly, Cherenkov radiation-induced hyperthermia should be considered a complementary rather than a standalone therapeutic modality. Mild hyperthermia in the range of 41–45 °C is well established to enhance tumor radiosensitivity and potentiate radiation-induced cytotoxicity, whereas higher temperatures exceeding 50–60 °C may lead to direct thermal cytotoxicity and localized tumor ablation. Therefore, the heat generated through local absorption of Cherenkov radiation can synergistically amplify the therapeutic efficacy of radionuclide therapy by simultaneously delivering ionizing radiation and spatially confined thermal enhancement within the tumor volume. Future studies should explore optimizing radionuclide selection and activity levels to maximize therapeutic temperature windows while minimizing unwanted heating in surrounding healthy tissue.

## 5. Conclusion

This study provides the first Monte Carlo-based investigation of Cherenkov radiation-induced hyperthermia in hepatic tumor radionuclide therapy across a range of beta-emitting radionuclides. Our findings highlight the potential of radionuclides such as <sup>32</sup>P and <sup>90</sup>Y as therapeutic radiation sources and as in situ heat generators via Cherenkov absorption. The observed temperature elevations, which range from mild hyperthermia to levels sufficient for direct cytotoxic effects and even thermal ablation, suggest that Cherenkov-induced heating can significantly enhance the therapeutic efficacy of radionuclide therapy, particularly when high-energy beta-emitting radionuclides are used. The spatially confined nature of this heating, driven by the tissue's optical properties and localized energy deposition, offers a valuable strategy for tumor-targeted hyperthermia. Combined with the known radiosensitizing effects of hyperthermia, these results support the integration of Cherenkov-driven thermal mechanisms into the design of future theranostic radiopharmaceuticals. Further experimental and clinical research is warranted to validate these findings and to optimize

radionuclide selection, dosing, and delivery timing for maximal clinical benefit.

## Acknowledgments

The Tabriz University of Medical Sciences, Tabriz, Iran, supported this work. Under the research ethics certificate, IR.TBZMED.VCR.REC.1403.247.

This study has been supported by the Deputy of Research at Tabriz University of Medical Sciences, Tabriz, Iran [Grant # 75027].

## References

- 1- L. Tselikas and M. Ronot, "Trans-Arterial Radioembolisation for HCC: Personalised Dosimetry Beyond Yttrium 90." (in eng), *Liver Int*, Vol. 45 (No. 4), p. e16184, Apr (2025).
- 2- D. Boshell and L. Bester, "Radioembolisation of liver metastases." (in eng), *J Med Imaging Radiat Oncol*, Vol. 67 (No. 8), pp. 842-52, Dec (2023).
- 3- M. A. Vente, M. G. Hobbelenk, A. D. van Het Schip, B. A. Zonnenberg, and J. F. Nijsen, "Radionuclide liver cancer therapies: from concept to current clinical status." (in eng), *Anticancer Agents Med Chem*, Vol. 7 (No. 4), pp. 441-59, Jul (2007).
- 4- Y. Anbari et al., "Current status of yttrium-90 microspheres radioembolization in primary and metastatic liver cancer." (in eng), *J Interv Med*, Vol. 6 (No. 4), pp. 153-59, Nov (2023).
- 5- Omar Desouky, Nan Ding, and Guangming Zhou, "Targeted and non-targeted effects of ionizing radiation." *Journal of Radiation Research and Applied Sciences*, Vol. 8 (No. 2), pp. 247-54, 2015/04/01/ (2015).
- 6- Saurabh Saini and Prajwal Gurung, "A comprehensive review of sensors of radiation-induced damage, radiation-induced proximal events, and cell death." *Immunological Reviews*, Vol. 329 (No. 1), p. e13409, (2025).
- 7- Michael Hausmann, Myriam Schäfer, Martin Falk, Iva Falková, Jiri Toufar, and Lucie Toufarová, "Deciphering Chromosomal Translocation Mechanisms: The Influence of Radiation Type and Chromatin Architecture." in *Chromosomal Abnormalities - From DNA Damage to Chromosome Aberrations*, Sonia Soloneski, Ed. Rijeka: *IntechOpen*, (2025).
- 8- Robert N. C. Pfeifer and Timo A. Nieminen, "Visualization of Čerenkov radiation and the fields of a moving charge." *European Journal of Physics*, Vol. 27 (No. 3), p. 521, 2006/03/15 (2006).
- 9- R. K. Gill, G. S. Mitchell, and S. R. Cherry, "Computed Čerenkov luminescence yields for radionuclides used in

- biology and medicine." (in eng), *Phys Med Biol*, Vol. 60 (No. 11), pp. 4263-80, Jun 7 (2015).
- 10- Justin S. Klein, Conroy Sun, and Guillem Pratx, "Radioluminescence in biomedicine: physics, applications, and models." *Physics in Medicine & Biology*, Vol. 64 (No. 4), p. 04TR01, 2019/02/07 (2019).
- 11- Adam K. Glaser, Rongxiao Zhang, David J. Gladstone, and Brian W. Pogue, "Optical dosimetry of radiotherapy beams using Cherenkov radiation: the relationship between light emission and dose." *Physics in Medicine & Biology*, Vol. 59 (No. 14), p. 3789, 2014/06/18 (2014).
- 12- Parwane Parsa, Steven L. Jacques, and Norman S. Nishioka, "Optical properties of rat liver between 350 and 2200 nm." *Applied Optics*, Vol. 28 (No. 12), pp. 2325-30, 1989/06/15 (1989).
- 13- J. Crezee, N. A. P. Franken, and A. L. Oei, "Hyperthermia-Based Anti-Cancer Treatments." (in eng), *Cancers (Basel)*, Vol. 13 (No. 6), Mar 12 (2021).
- 14- S. Jan *et al.*, "GATE: a simulation toolkit for PET and SPECT." (in eng), *Phys Med Biol*, Vol. 49 (No. 19), pp. 4543-61, Oct 7 (2004).
- 15- S. Agostinelli *et al.*, "Geant4—a simulation toolkit." *Nuclear Instruments and Methods in Physics Research Section A: Accelerators, Spectrometers, Detectors and Associated Equipment*, Vol. 506 (No. 3), pp. 250-303, 2003/07/01/ (2003).
- 16- V. Cuplov, F. Pain, and S. Jan, "Simulation of nanoparticle-mediated near-infrared thermal therapy using GATE." (in eng), *Biomed Opt Express*, Vol. 8 (No. 3), pp. 1665-81, Mar 1 (2017).
- 17- S. Chauvie *et al.*, "Geant4 low energy electromagnetic physics." in *IEEE Symposium Conference Record Nuclear Science 2004.*, (2004), Vol. 3, pp. 1881-85 Vol. 3.
- 18- Erik Dietz-Laursonn, "Peculiarities in the Simulation of Optical Physics with Geant4." *arXiv: Instrumentation and Detectors*, (2016).
- 19- B. Đurnić, A. Potylitsyn, A. Bogdanov, and S. Gogolev, "On the rework and development of new Geant4 Cherenkov models." *Journal of Instrumentation*, Vol. 20 (No. 02), p. P02008, 2025/02/11 (2025).
- 20- W. P. Segars, B. M. W. Tsui, Cai Jing, Yin Fang-Fang, G. S. K. Fung, and E. Samei, "Application of the 4-D XCAT Phantoms in Biomedical Imaging and Beyond." (in eng), *IEEE Trans Med Imaging*, Vol. 37 (No. 3), pp. 680-92, Mar (2018).
- 21- Marzieh Amani, Ali Bavali, and Parviz Parvin, "Optical characterization of the liver tissue affected by fibrolamellar hepatocellular carcinoma based on internal filters of laser-induced fluorescence." *Scientific Reports*, Vol. 12 (No. 1), p. 6116, 2022/04/12 (2022).
- 22- Franklin C Wong, "MIRD: radionuclide data and decay schemes." *Journal of Nuclear Medicine*, Vol. 50 (No. 12), pp. 2091-91, (2009).
- 23- H. H. Pennes, "Analysis of tissue and arterial blood temperatures in the resting human forearm." (in eng), *J Appl Physiol*, Vol. 1 (No. 2), pp. 93-122, Aug (1948).
- 24- E. H. Wissler, "Pennes' 1948 paper revisited." (in eng), *J Appl Physiol (1985)*, Vol. 85 (No. 1), pp. 35-41, Jul (1998).
- 25- Y Kim, "Insight segmentation and registration toolkit." *The National Library of Medicine: Washington, DC, USA*, (2001).
- 26- Roger W Pryor, Multiphysics modeling using COMSOL®: a first principles approach. *Jones & Bartlett Publishers*, (2009).
- 27- G. Yona, N. Meitav, I. Kahn, and S. Shoham, "Realistic Numerical and Analytical Modeling of Light Scattering in Brain Tissue for Optogenetic Applications(1,2,3)." (in eng), *eNeuro*, Vol. 3 (No. 1), Jan-Feb (2016).
- 28- Harley Harris Ross, "Measurement of .beta.-emitting nuclides using Cherenkov radiation." *Analytical Chemistry*, Vol. 41 (No. 10), pp. 1260-65, 1969/08/01 (1969).
- 29- C. T. Germer *et al.*, "Optical properties of native and coagulated human liver tissue and liver metastases in the near infrared range." (in eng), *Lasers Surg Med*, Vol. 23 (No. 4), pp. 194-203, (1998).
- 30- I. Carneiro, S. Carvalho, R. Henrique, L. Oliveira, and V. Tuchin, Measurement of optical properties of normal and pathological human liver tissue from deep-UV to NIR. (*SPIE Photonics Europe*). *SPIE*, (2020).
- 31- Barbara Dukic *et al.*, "Mild Hyperthermia-Induced Thermogenesis in the Endoplasmic Reticulum Defines Stress Response Mechanisms." *Cells*, Vol. 13 (No. 13), p. 1141, (2024).
- 32- H. Gregory and K. A. Weant, "Pathophysiology and Treatment of Malignant Hyperthermia." (in eng), *Adv Emerg Nurs J*, Vol. 43 (No. 2), pp. 102-10, Apr-Jun 01 (2021).
- 33- B. Hildebrandt *et al.*, "The cellular and molecular basis of hyperthermia." (in eng), *Crit Rev Oncol Hematol*, Vol. 43 (No. 1), pp. 33-56, Jul (2002).
- 34- Xiaofei Jin *et al.*, "Temperature control and intermittent time-set protocol optimization for minimizing tissue carbonization in microwave ablation." *International Journal of Hyperthermia*, Vol. 39 (No. 1), pp. 868-79, 2022/12/31 (2022).
- 35- C. J. Diederich, "Thermal ablation and high-temperature thermal therapy: overview of technology and clinical implementation." (in eng), *Int J Hyperthermia*, Vol. 21 (No. 8), pp. 745-53, Dec (2005).

- 36- S. Kwon, S. Jung, and S. H. Back, "Combination Therapy of Radiation and Hyperthermia, Focusing on the Synergistic Anti-Cancer Effects and Research Trends." (in eng), *Antioxidants (Basel)*, Vol. 12 (No. 4), Apr 13 (2023).
- 37- M. F. Righini, A. Durham, and P. G. Tsoutsou, "Hyperthermia and radiotherapy: physiological basis for a synergistic effect." (in eng), *Front Oncol*, Vol. 14p. 1428065, (2024).
- 38- Loïc Van Dieren *et al.*, "Combined Radiotherapy and Hyperthermia: A Systematic Review of Immunological Synergies for Amplifying Radiation-Induced Abscopal Effects." *Cancers*, Vol. 16 (No. 21), p. 3656, (2024).

PROOF